Published paper

Measurement of Excitation Winding Temperature on Synchronous Generator in Rotation Using Infrared Thermography

Stjepan Stipetic, *Student member, IEEE,* Marinko Kovacic, Zlatko Hanic, *Student member, IEEE,* Mario Vrazic, *Member, IEEE*

Abstract – **A new measurement method for infrared (IR) surface temperature measurement of excitation winding in rotation is presented. Method is experimentally verified on 400 kVA salient pole synchronous generator. This method uses an industrial infrared thermometer which represents an alternative to expensive fast infrared thermometers or cameras. Target application of this method is determination of the dynamic limit in the P-Q diagram of a synchronous generator due to excitation winding overheating. Measurement error model which shows the way how to minimize measurement error has also been derived. The effect of the interpolar surface can be cancelled if the IR thermometer is positioned at a certain angle with respect to machine's main axis. Digital temperature sensors have been mounted on the rotor to measure the excitation winding surface temperature for comparison.**

Index Terms – **Infrared image sensors, Infrared measurements, Monitoring, Rotating machines, Temperature measurement**

NOMENCLATURE

T_p - Absolute temperature of salient pole surface

T_{ip} - Absolute temperature of interpolar surface

T_d - Absolute temperature measured by IR thermometer (compensated)

ε_p - Emissivity of salient pole surface

ε_{ip} - Emissivity of interpolar surface

ε_d - Emissivity set on IR thermometer

I_p - Irradiance of salient pole surface

I_{ip} - Irradiance of interpolar surface

I_d - Irradiance read by IR thermometer sensor

S - IR target spot size diameter (Fig.5)

D - Distance between IR thermometer and object

R - Radius of IR thermometer position (Fig.5)

S_p, S_{ip} - Salient pole surface and interpolar surface on annulus defined by radius R-$S/2$ and R+$S/2$

o - Ratio of S_p and S_{ip}

ΔT - Temperature measurement error

ΔT_p - Difference between interpolar surface temperature and pole temperature

G_1, G_2 - Goal functions for minimization of measurement error

I. INTRODUCTION

During the past several years, infrared (IR) thermography [1], [2], [3] has become a powerful method for investigating thermal flow paths across complex geometries, for studying heat transfer or simply as a diagnostic tool for diverse applications [4], [5]. The use of an IR camera as a temperature sensor in convective heat transfer measurements appears advantageous, when compared to standard sensors, from several points of view. In standard techniques, where temperature is measured by thermocouples, resistance temperature detectors or pyrometers, the sensor yields the local heat flux at a single point (or a spatial averaged one). On the contrary, IR thermography is a completely non-intrusive method that provides two-dimensional temperature images [6].

Non-contact excitation winding temperature estimation based on resistance measurement has been widely used on synchronous generators for protection. It is an indirect method which gives only average temperature and is quite inaccurate due to slip ring nonlinear contact resistance. Nevertheless, methods for the temperature estimation of the induction machine stator and rotor winding were also developed [7], [8], [9]. They often use an injection of small low frequency or DC currents [10], and the analysis of the current and voltage frequency spectrum. Current injection may cause a certain unwanted magnetic phenomena in the induction machine [11]; which is not a case with the IR thermography.

Rotating collector (slip-ring) could also be used to bring the temperature signals (obtained by thermocouples) from rotating to static environment [13], [14]. When dealing with thermocouples and slip-rings special care must be taken to eliminate thermal voltage [14]. Nevertheless, in most cases it is not possible to add additional slip-rings on shaft of large machines in power plants. Since IR thermography enables noncontact temperature measurements it could be considered as advantage compared to contact slip-ring approach.

By using an IR optical fiber it is possible to measure temperature at hard to reach places without optical access inside of the machine, which makes the IR thermography very appropriate for diagnostics, protection and control [12]. However, researches in rotating environments are rarely reported, compared to stationary environments, mostly due to limited optical access and other problems associated with measuring techniques, data acquisition and data processing. Most reported studies in rotating environments have been

S. Stipetic, M. Kovacic, Z. Hanic and M. Vrazic are with Department of Electric Machines, Drives and Automation, Faculty of Electrical Engineering and Computing, University of Zagreb, Croatia (e-mail: stjepan.stipetic@fer.hr, marinko.kovacic@fer.hr, zlatko.hanic@fer.hr, mario.vrazic@fer.hr).

focused on local convective heat transfer and temperature mapping on the rotating disk in still air [4], [15], [16], the impinging jet on the rotating disk [4] or 180° turn rotating channel [4], [16].

Kral et. al. [17] used the IR sensor to measure the temperature of the rotor of 210 kW induction machine in rotation, but the results of measurement were given with caution, and served only for a rough comparison. Mori et. al. [6], [18] measured the temperature on a rotor blade with a fast IR camera. Budzer et. al. [19] measured the surface temperature of a rotating tire with a high-speed IR line camera. Pellé and Harmand [20] studied the heat transfer in a rotor stator system with an air gap by measuring the temperature of a rotating aluminum disk with IR camera. All methods proposed in those papers use expensive high speed IR cameras (for example: camera with maximum frame rate 150 Hz at integration time of 10 μs [6], [18]) to obtain 2D temperature field image. This paper deals with the methods for the IR temperature measurement on a synchronous generator excitation winding in rotation using the low cost IR industrial thermometer. Thermometer output is not the 2D temperature field but spatially averaged temperature. Nevertheless it is possible to obtain the surface temperature with satisfying accuracy using the proposed methods [43].
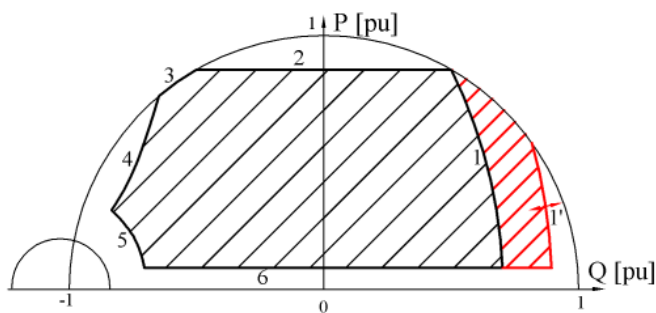
1. Static limit caused by excitation winding overheating
1'. Dynamic limit due to excitation winding overheating
2. Static limit caused by maximal turbine active power
3. Static limit caused by armature winding overheating
4. Practical stability static limit
5. Minimal excitation current static limit
6. Static limit caused by minimal turbine active power

Fig.1 – P-Q (capability) diagram

Synchronous generators have an operational limit due to excitation winding overheating. All operational limits are shown in the P-Q (capability) diagram (Fig.1). Synchronous generator manufacturers usually define static P-Q diagrams with static limits. The manufacturers guarantee safe and permanent operation without failure in the static operational area defined by the static limits. The operational area of a P-Q diagram has a certain amount of built-in redundancy. On the other hand, if a machine starts from a cold state, it can operate under an overload during a short period of time until, for example, it reaches its operational temperature. Thus an excitation winding can be overloaded until it reaches its nominal temperature. In that case, a synchronous generator can operate outside of the operational area defined by the static P-Q diagram [21], [22]. Of course, a synchronous generator cannot be overloaded at will, but with respect to temperature, stability etc. It means that short-time overload limits change in time. They are called dynamic limits and a P-Q diagram with dynamic limits is called a dynamic P-Q diagram. In order to determine the dynamic limit caused by the heating of an excitation winding

in a certain moment, it is necessary to have reliable information on the winding temperature (i.e. maximum temperature of copper and insulation of the excitation winding). An IR thermometer measures only surface temperature but FEA ([24]-[29]) or lumped ([30]-[14]) thermal model of a generator (particularly salient pole with an excitation winding) can be used to determine the critical insulation temperature which appears at the copper-insulation contact. This paper presents a method for acquiring surface temperature which can be used as one of the input signals in order to enhance accuracy of those models.

II. INFRARED MEASUREMENT

A. Physical Background

The Stefan–Boltzmann law states that the total energy radiated per unit surface area of a black body in unit time, I, is directly proportional to the fourth power of the black body's absolute temperature T. In various literatures, I is named the black-body irradiance, energy flux-density, radiant flux, thermal-flux, or emissive power.

$$I = \sigma \cdot T^4 \qquad (1)$$

The constant of proportionality is σ, called the Stefan–Boltzmann constant, has a value of

$$\sigma = 5.6704 \cdot 10^{-8} \ \text{W/m}^2\text{K} \qquad (2)$$

A more general case is of a grey body, the one that doesn't absorb or emit the full amount of irradiance. Instead, it radiates a portion of it, characterized by its emissivity, ε:

$$I = \varepsilon \cdot \sigma \cdot T^4 \qquad (3)$$

Emissivity of a given body surface is a function of angle of observation α, wavelength λ, body temperature T and time t.

When the application of IR thermography on this specific problem is being considered, some of these effects can be neglected while measuring surface temperature of a synchronous generator excitation winding [1], [2]. The effect of time on emissivity is important only for ultrafast thermal processes, and the change of excitation winding surface temperature is a rather slow. Maximum allowed copper-insulation contact temperature for the insulation class F is 155 °C but almost all the large machines built for class F have allowed maximum temperature for class B (130 °C). Surface temperature is definitely lower than temperature on copper-insulation contact. The expected surface temperatures are within the range from the ambient temperature when a generator is in a cold state (20 °C) to the maximum 120 °C.

Literature states that the excitation winding surface emissivity (non-metal oil paint or varnish-paint) is constant in the temperature range from 0 °C to 100 °C and the spectrum range from 8 to 14 μm (Long-wave, LW spectrum) [1], [2]. Typical emissivity values are 0.92 - 0.96 for this common type of paint. There are no data for emissivity at temperatures above 100 °C. A slight decrease in emissivity values can be expected but due to the fact that temperature depends on fourth root of emissivity, the effect can be neglected from accuracy point of view.

For opaque bodies transmissivity equals zero. As the pole of synchronous generator is opaque, very high emissivity ε

means that the reflectivity r is very small. In that case following equation can be written:

$$\varepsilon + r = 1 \qquad (4)$$

Very small reflectivity means that radiation radiated by other bodies and reflected from the observed surface for this application can be neglected.

According to Wien's displacement law, the wavelength range of the maximum radiation intensity for the temperature range between 0 and 150°C is within 8 to 14 μm. Instead of integration in the whole spectra, sensor is able to collect only radiation in its spectral response interval (8 to 14 μm). Limited wavelength response decreases thermal flux in non-linear way and the Stefan-Boltzmann law for black body becomes:

$$I = \varepsilon \cdot \sigma \cdot T^n \qquad (5)$$

where ε ranges from 0 to 1, and n ranges between 3 and 4 [41]. Power n is chosen to fit correlation between irradiance and measuring temperature in particular spectral interval.

Taking into account the equipment used for this purpose (commercial infrared sensor) the radiation outside the sensor spectral response interval in desired temperature range can be neglected.

Due to the previous discussion, it can be stated that the emissivity for this application is only a function of angle of observation.

B. IR thermometer

The IR thermometer used for the measurement (Fig.2) is an industrial sensor with a thermopile detector. The specifications are listed in table I.

Fig.2 – IR thermometer

Thermopile detectors are built as a system of thermocouples connected in a series. A measurement junction (hot junction) is connected to a photosensitive element exposed to infrared radiation, while a reference junction (cold junction) is placed on a heat sink, which is near the ambient temperature. Thermopiles do not measure the absolute temperature, but generate an output voltage proportional to a local temperature difference. The output of a thermopile is usually in the range of tens or hundreds of millivolts. The infrared device may be used to provide spatial temperature averaging.

The principle of operation of the IR thermometer is described as follows. Irradiated energy heats the absorption material thermally coupled to the thermocouples, the temperature difference between the hot and cold junction generates a voltage which is proportional to the difference between the sensor ambient temperature and the absorber temperature. In order to measure absolute temperature of an

object IR thermopile detectors have a conventional temperature sensor which measures the cold junction temperature. It is converted to the temperature using Stefan-Boltzmann law and the known emissivity of the object. The temperature is afterwards averaged if needed (averaging time can be modified in the sensor's software).

TABLE I
TECHNICAL SPECIFICATIONS OF IR THERMOMETER

Temperature range	-18 to 500 °C
Optical resolution (90 %), D/S	15:1
Spectral response	8 to 14 μm
Accuracy	± 1 % of reading or ± 1.4 °C, whichever is greater
Repeatability	± 0.5 % of reading or ± 0.7 °C, whichever is greater
Detector	Micromachined thermopile
Response time (95 %)	165 ms
Temperature resolution	0.1 K

The industrial thermopile detector used in experiments has the time constant of 55 ms which is 1/3 of the response time based on 95% received energy (165 ms). The sampling time of the detector output signal is 25 ms.

The optical diagram (Fig.3) of the infrared thermometer indicates the target spot diameter (S) at any given distance (D) between the target object and the sensing head. All target spot sizes indicated in the optical diagrams are based on 90% energy. It means that the thermometer measures the average temperature of a circle (spot). When placing and pointing the thermometer, attention must be paid on the ratio between the spot size on a given distance and the size of the observed object.
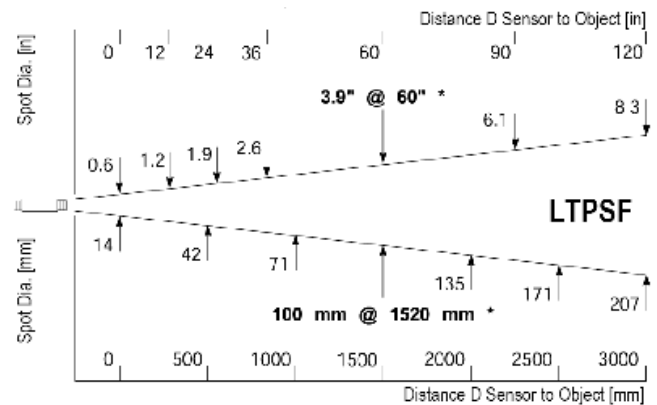

Fig.3 – Optical diagram

C. IR Measurement in Rotation

Several facts have to be considered when measuring the surface temperature of an excitation winding in rotation (Fig.6). Due to high emissivity of the observed surfaces, low ambient temperature and clear atmosphere, the reflected radiation and atmospheric absorption are neglected in order to simplify the mathematical model of a thermometer. Further analysis is carried out with the assumption that the IR thermometer is pointed perpendicularly on the surface of a pole (parallel to the machine's axis).

The observer (IR thermometer) distinguishes two different surfaces in terms of infrared radiation: an excitation winding placed on a salient pole and an interpolar surface (Fig.4, Fig.5). The space between the salient poles can include mechanical elements for the fixation of the salient poles and winding. Due to rotation, the IR thermometer

absorbs thermal radiation from the excitation winding on the salient pole and from the interpolar surface as well (Fig.5).

Fig.4 – View on the rotor of the observed generator

Temperature measured by the IR thermometer depends on rotation speed and response time of a thermopile detector because temperature and emissivity of an excitation winding surface and interpolar surface are not equal in general. If detector is rather fast with respect to rotation speed, the thermopile detector can distinguish irradiation from the pole and interpolar surface and one can see a periodic change in output temperature. On the contrary, if the detector is slow with respect to rotational speed, it reads the average irradiance of a rotor.

A more sophisticated (faster) infrared sensor could be used with the synchronous detector in order to determine the alternation of surfaces. The aim of this paper is to present the methodology of measuring alternating rotating surface temperature with rather slow infrared sensor.

The observed generator has the nominal speed of 1000 rpm (50 Hz, 6 poles). One pair of the pole and interpolar surface takes 10 ms to pass in front of the thermometer, and during the response time of 165 ms the rotor makes 2.75 turns.
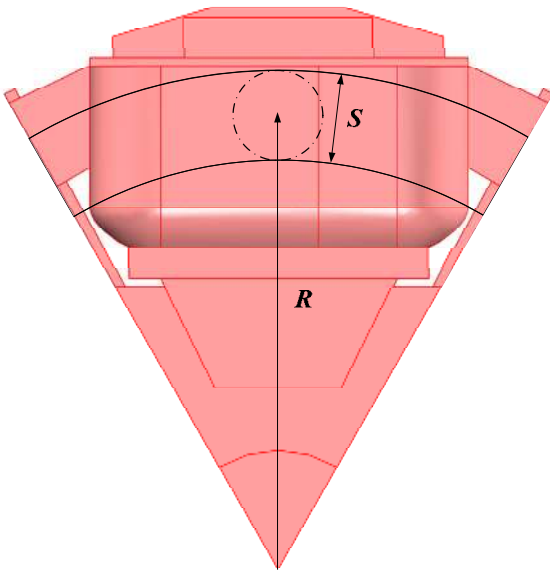

Fig.5 – Definition of radius R and spot size S. Hatched area is observed by IR thermometer in rotation

The following equations can be set for a simplified model of the IR thermometer (slow response time compared to speed of rotating object) which measures temperature of the rotor of synchronous generator in rotation:

$$I_d = \frac{I_p \cdot S_p + I_{ip} \cdot S_{ip}}{S_p + S_{ip}} = \frac{I_p \cdot o + I_{ip}}{o+1} \tag{6}$$

Ratio o can be determined from the geometry of the rotor knowing distance D and radius R. It depends on machine's rotor design and the position of the IR thermometer. By assuming that IR thermometer has the temperature compensation, and by applying Stefan-Boltzmann's law on (4) we get:

$$\varepsilon_d \sigma T_d^4 = \frac{\varepsilon_p \sigma T_p^4 \cdot o + \varepsilon_{ip} \sigma T_{ip}^4}{o+1} \tag{7}$$

The temperature measured by the IR thermometer is given by (8)

$$T_d = \sqrt[4]{\frac{\varepsilon_p T_p^4 \cdot o + \varepsilon_{ip} T_{ip}^4}{\varepsilon_d (o+1)}} \tag{8}$$

It is a function of the emissivity and temperature of the pole surface, interpolar surface and ratio o.

For more detailed model one can substitute (5) into (6) instead Stefan-Boltzman equation. In that case device temperature can be derived as follows:

$$T_d = \left(\frac{\varepsilon_p T_p^n \cdot o + \varepsilon_{ip} T_{ip}^n}{\varepsilon_d (o+1)} \right)^{\frac{1}{n}} \tag{9}$$

For further discussion parameter n will be set to 4, i.e. (8) will be used.

D. *Emissivity Setting And Error Analysis*

Particular attention had to be paid to setting device emissivity ε_d. It is relatively easy to determine the emissivity for the pole surface and interpolar surface when the rotor is in standstill with the conventional temperature measurement. One can use a sticker or paint of known emissivity on the observed surface or place a temperature sensor to measure surface temperature. When determining correct emissivity, the IR device and conventional temperature sensor (thermocouple, RTD probe, digital IC probe, etc.) have to give equal temperature output. One of possible choices is to adjust the device emissivity while a machine is in thermal equilibrium (i.e. in a cold state). In that case the temperature of the pole surface is equal to the temperature of the interpolar surface. If pole and interpolar surface are in thermal equilibrium also in rotation, device emissivity ε_d can be set to the value according to (7):

$$\varepsilon_d = \frac{\varepsilon_p \cdot o + \varepsilon_{ip}}{(o+1)} \tag{10}$$

Due to the same temperature of the pole and the interpolar surface ($T_p = T_{ip}$), IR thermometer will measure the same temperature in rotation and in standstill.

$$T_d = \sqrt[4]{\frac{\varepsilon_p T_p^4 \cdot o + \varepsilon_{ip} T_p^4}{\varepsilon_d (o+1)}} = \sqrt[4]{\frac{\varepsilon_p \cdot o + \varepsilon_{ip}}{\varepsilon_d (o+1)} T_p^4} = T_P \tag{11}$$

As the excitation winding heats, its temperature in general differs from the temperature of the elements in interpolar space. The IR thermometer will measure temperature according to (8), but the aim is to measure the pole temperature correctly.

To ensure the correct pole temperature measurement with the IR thermometer, the effect of the term $\varepsilon_{ip}T_{ip}^4$ in (8) should be cancelled or substantially reduced. Some terms in (11) can be neglected for large ratio o. In that case, by setting device emissivity equal as pole emissivity, we get:

$$T_d = \sqrt[4]{\frac{\varepsilon_p T_p^4 + \dfrac{\varepsilon_{ip}T_{ip}^4}{o}}{\varepsilon_d\left(1+\dfrac{1}{o}\right)}} = \sqrt[4]{\frac{\varepsilon_p T_p^4 + \dfrac{\varepsilon_{ip}T_{ip}^4}{o}}{\varepsilon_p\left(1+\dfrac{1}{o}\right)}} = T_p \qquad (12)$$
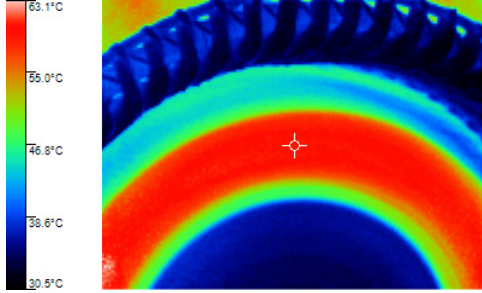

Fig.6 – Thermal image of excitation winding in rotation (IR camera) with long exposition compared to rotor speed

By introducing difference between interpolar surface temperature and pole surface temperature ΔT_p,

$$\Delta T_p = T_{ip} - T_p \qquad (13)$$

measurement error ΔT (difference between pole surface temperature and measured temperature) can be expressed as:

$$\Delta T = T_p - T_d = T_p - \sqrt[4]{\frac{\varepsilon_p T_p^4 \cdot o + \varepsilon_{ip}\left(T_p + \Delta T_p\right)^4}{\varepsilon_d(o+1)}} \qquad (14)$$

For most hydro-generators (slower than 500 rpm), parameter o is significant (30 or higher), therefore the effect of irradiation radiated from the interpolar surface can be neglected as shown on Fig. 7. (satisfactory small measurement error ΔT can be achieved). Excitation winding of such generator is shown on Fig. 8
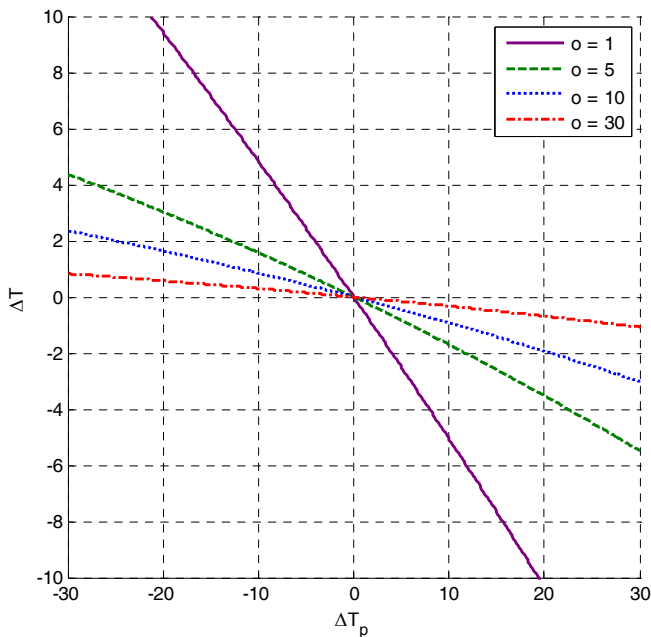

Fig. 7 Measurement error for various o and ΔT_p
($\varepsilon_{ip} = 0.9$, $\varepsilon_p = 0.93$, ε_d according to formula (10), $T_d = 333\ K\ (60\ °C)$)

Fig. 8 - View on the rotor of the generator in Hydro Power Plant HE "Vinodol" ($o = 40$)

Emissivity could be set to obtain measurement error ΔT equal to zero for particular pole temperature and particular temperature difference ΔT_p (i.e. for nominal operating point.)

$$\varepsilon_d = \frac{\varepsilon_p \cdot o \cdot T_p^4 + \varepsilon_{ip} \cdot \left(T_p + \Delta T_p\right)^4}{(o+1) \cdot T_p^4} \qquad (15)$$

Also, for a certain pole temperature, or for a certain range of pole and interpolar surface temperatures, the device emissivity can be set to minimize the deviation between the pole temperature and temperature measured by the IR thermometer.

For a given pole temperature T_p and for certain range of temperature differences $\Delta T_{p\ min}$ and $\Delta T_{p\ max}$, emissivity can be set to minimize goal function:

$$G_1(\varepsilon_d; T_p) = \int_{\Delta T_{ip\ min}}^{\Delta T_{ip\ max}} \Delta T^2(T_p, \Delta T_{ip})\,d(\Delta T_{ip}) \rightarrow \text{min!} \qquad (16)$$

Similarly, for a given range of pole temperatures $T_{p\ min}$ and $T_{p\ max}$ and for certain range of temperature differences $\Delta T_{p\ min}$ and $\Delta T_{p\ max}$, emissivity can be set to minimize goal function:

$$G_2(\varepsilon_d) = \int_{T_{p\ min}}^{T_{p\ max}} \int_{\Delta T_{ip\ min}}^{\Delta T_{ip\ max}} \Delta T^2(T_p, \Delta T_{ip})\,d(\Delta T_{ip})\,d(T_p) \rightarrow \text{min!} \qquad (17)$$
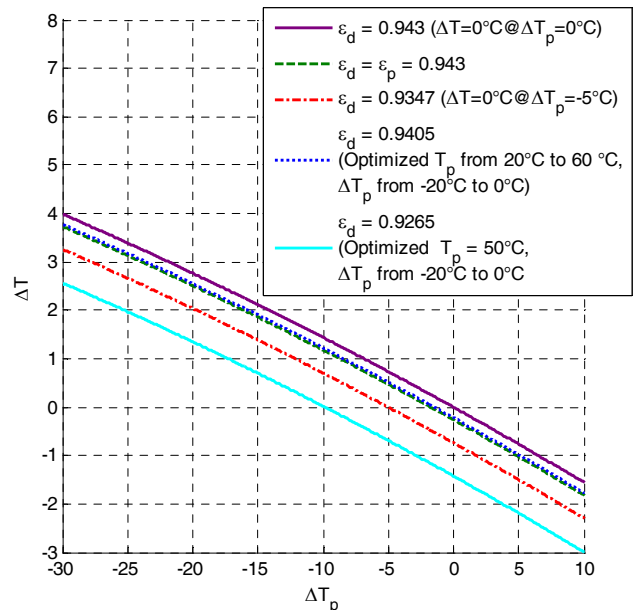

Fig. 9 Measurement error ΔT dependence on ΔT_p for various ε_d for $\varepsilon_p = 0.94$, $\varepsilon_{ip} = 0.96$ and $o = 5.8$

Fig. 9 shows measurement error dependence on ΔT_p for the observed generator with various emissivity setups. The value of parameter o for tested generator is 5.8, polar and interpolar emissivities were 0.94 and 0.96, respectively.

E. Interpolar surface Effect Cancelling

Lambert's law states that irradiance of a flat surface is the same in all directions. The effect of irradiation radiated from the interpolar surface can therefore be disregarded if the IR thermometer is directed to the excitation winding by a certain angle with respect to the machine main axis. In that case the IR thermometer reads only the irradiance of the excitation winding pole surface because due to geometry and rotation, the interpolar surface cannot radiate towards the thermometer, it produces the same effect as increasing of the ratio o towards the infinity.

The temperature of the excitation winding surface on the salient pole sides differs from the temperature on the frontal surface because of different ventilation conditions, but the difference is negligible, especially in case of forced air cooling. The emissivity of the surface varies according to the angle of observation, but does not change significantly for the angles between 0° and 45° [1], [6]. Emissivity for a certain angle of view can be determined when a rotor is in standstill.

III. RESULTS

A. Reference Temperature Measurement

The wireless acquisition system was also developed and it can be used for "on-line" data acquisition of the excitation winding surface temperature even during rotation Fig. 10 [42].
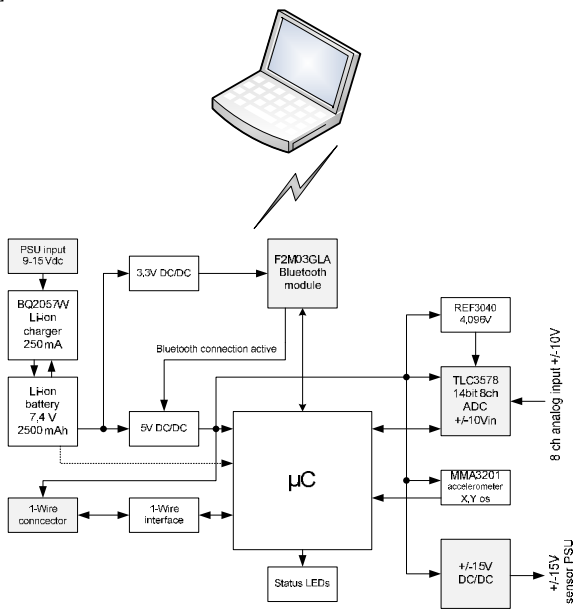

Fig. 10 - Block diagram of wireless measurement system

It uses modified, high precision digital temperature probes DS18S20, connected by the 1-Wire® interface to the Bluetooth® module. The total of 26 probes were mounted on the excitation winding surface with thermal conductive epoxy metal glue which assures accuracy, mechanical fixation and a small time constant of the probes themselves Fig.11. The system was thoroughly tested and the

methodology for preparation, wiring and mounting of DS probes has been determined. The obtained results were compared to the readings from class A Pt1000 probes (generally used in electrical machinery design). Excellent matching was found, both in a steady-state and dynamics. This wireless system was used to verify the IR temperature measurements. The accuracy of the digital probes is ± 0.5 °C.
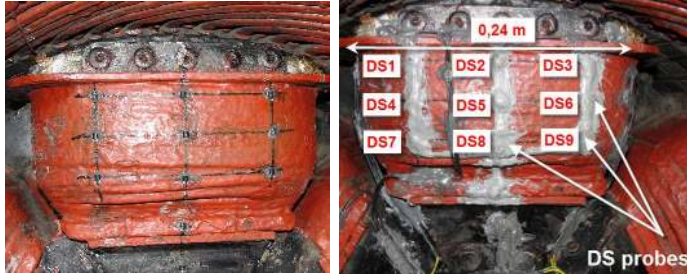

Fig.11 – DS probes mounted on excitation winding

The application for probe data acquisition was made in National Instruments LabVIEW. Temperatures of each sensor together with time base are logged in a textual file which is used for further analysis. Application has an option of rendering 3D surface temperature distribution based on temperatures collected from the probes and their position on the imported salient pole 3D model Fig. 12.
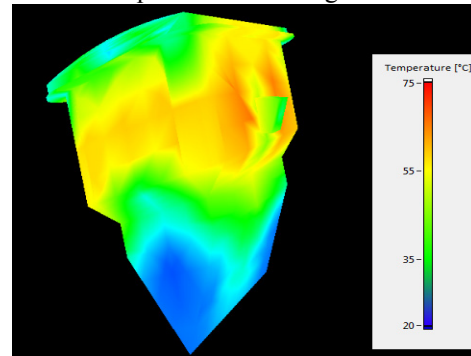

Fig. 12 - Surface temperature distribution over observed salient pole

B. Experiments

The experimental model included a synchronous hydro-generator (400 kVA, 400 V, 1000 rpm) with 24 DS probes mounted on one salient pole, one probe mounted on interpolar surface and one DS probe mounted on the adjacent control pole. Wireless measurement system is mounted on the rotor. It routes data from temperature sensors and wirelessly send them to computer. Temperature is also measured with IR thermometer (Fig. 13).
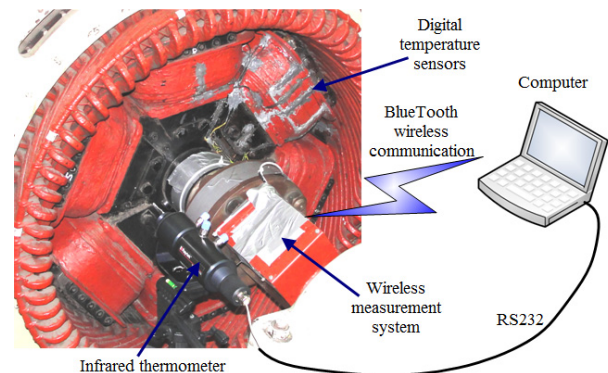

Fig. 13 – The experimental setup

The experiments included heating and cooling of the excitation winding in standstill and in rotation with various positions and a setup of the IR thermometer (angle, distance and emissivity). The emissivity for a certain angle has been calibrated when the rotor was in standstill by using standard thermography procedures. Readings from the IR thermometer are compared to the readings of DS probes mounted on the frontal surface and nearest to the thermometer spot place.

The following experiments have been conducted (Parameters are shown in table II, ground plan of experiment setup on Fig.14. and the results are presented on Fig.15 to Fig.21):

1. Heating of the excitation winding with a constant current (40 A), first in standstill, afterwards in rotation, which was followed by cooling in rotation. IR thermometer is positioned 45° with the respect of the machine's main axis.
2. Heating of the excitation winding with a constant current (45 A) during rotation. IR thermometer is positioned 45° with the respect of the machine's main axis.
3. Heating of the excitation winding with a constant current (40 A), first in standstill, afterwards in rotation. IR thermometer is positioned parallel with the machine's main axis.
4. Heating of the excitation winding with a constant current (40 A) during rotation. IR thermometer is positioned parallel with the machine's main axis.

If the experiment involves measurement in standstill, the infrared thermometer reading is compared with the reading of the DS5 probe (the central probe, nearest to the thermometer spot position). In the case of the measurement in rotation, the infrared thermometer reading is compared with the average reading of the 6 frontal probes (DS4 to DS9 or DS1 to DS6) placed on the spot trace. The temperature difference at the start of rotation must not be considered due to the time constant of the DS probes. Namely, the surface temperature of the excitation winding decreases immediately with the start of rotation because of increased convective heat transfer. The temperature of the sensor in the DS probes lags a certain amount of time due to the nature and encapsulation of the sensor.

TABLE II
PARAMETERS OF EXPERIMENTS

Experiment Number	1	2	3	4
Distance (D), m	0.37	0.60	0.92	0.32
Spot size (S), cm	2.5	4.0	6.0	2.1
Angle, °	45	45	0	0
Emissivity	0.94	0.93	0.94	0.94

The accuracy of the measurement system (IR thermometer + wireless data acquisition system with DS probes) can be roughly estimated to ± 2 °C.

The first experiment (Fig.15, Fig.16) shows a very good match in standstill as well as in rotation with a temperature difference smaller than the accuracy of the IR thermometer and the measurement system itself. As it has been said previously, a major difference in temperature reading at the start of rotation was caused by the different time constant between the thermopile device and the DS probe.
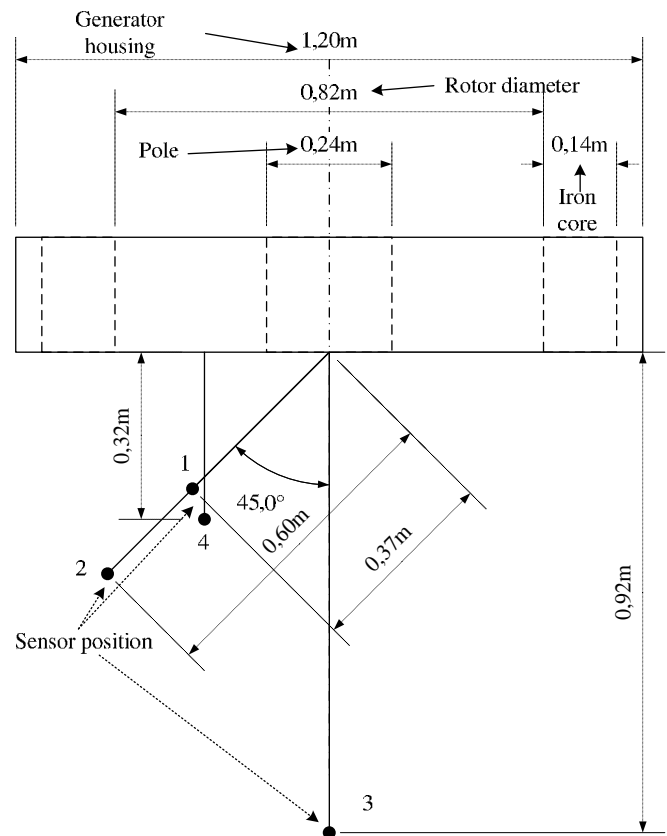

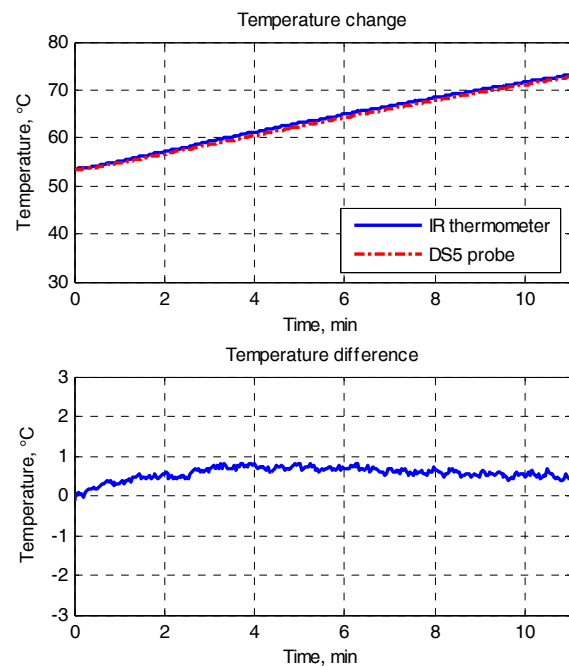Fig.14 – Ground plan of experiment setup

Fig.15 – Heating in standstill, experiment 1

The second experiment (Fig.17) shows an excellent match in rotation. The IR thermometer was placed on a larger distance than in the previous experiment, which leads to an increased spot size. Both the distance and spot size define an amount surface area viewed at a certain angle, so the calibration of emissivity for this experiment resulted in a slightly different emissivity factor, 0.93. Ambient temperature (reference temperature of the IR thermometer) is also shown on the graph. The temperature difference is again smaller than the accuracy of the IR thermometer.
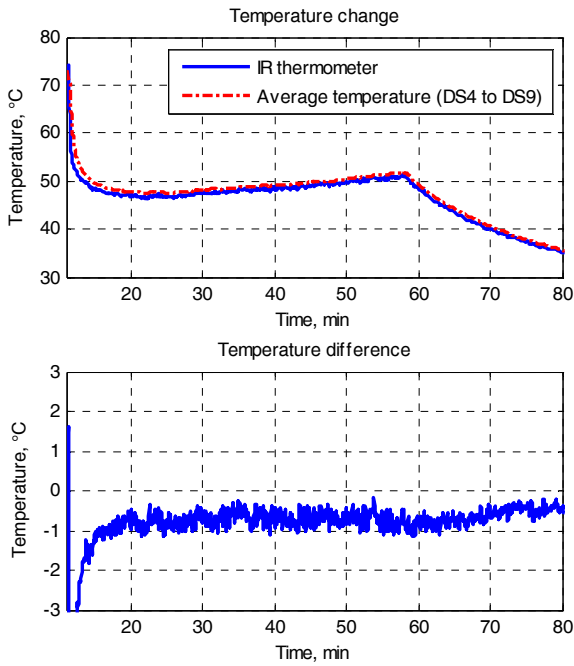
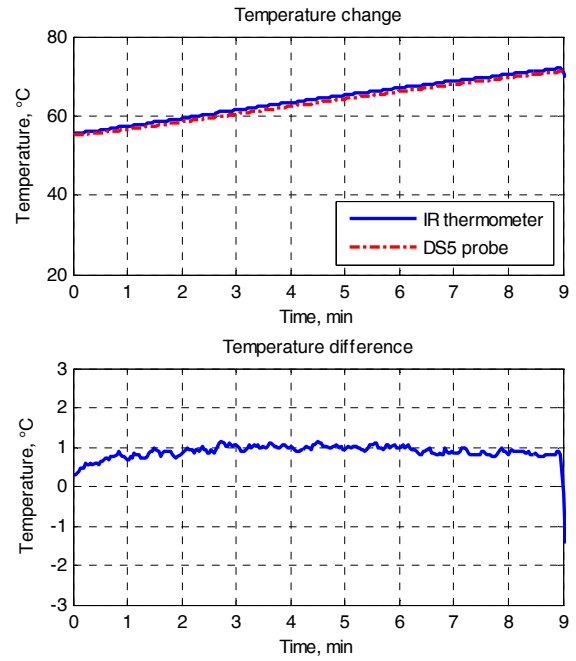Fig.16 – Heating and cooling in rotation, experiment 1
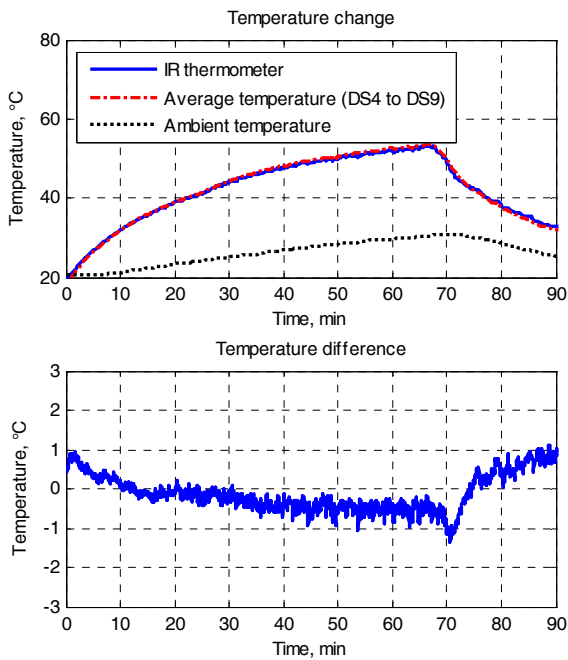

Fig.18 – Heating in standstill, experiment 3

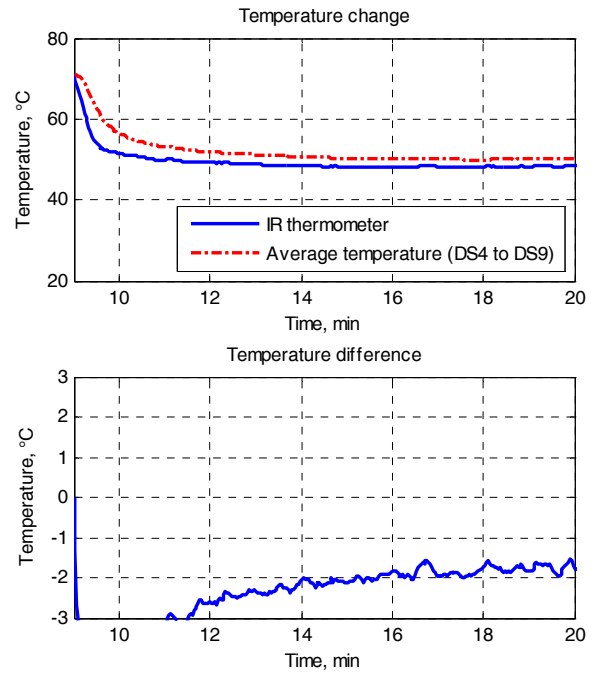Fig.17 – Heating and cooling in rotation, experiment 2

Fig.19 – Cooling in rotation, experiment 3

The third experiment (Fig.18, Fig.19) shows how even frontal placement of the IR thermometer can result in satisfactory accuracy. The spot was larger, due to a larger distance, and the radius of the IR thermometer position was carefully chosen to minimize the interpolar effect. The temperature difference also tends to be smaller due to slow equalization of the pole and interpolar temperature.

In the forth experiment IR thermometer was placed frontally, parallel to the machine main axis. Experiment includes measurement of the interpolar surface temperature (Fig.20) which enables measurement of error ΔT and interpolar space temperature and pole temperature difference ΔT_p. Fig.21 clearly shows increase of the measurement error ΔT with the increase of ΔT_p, as it was predicted with (14).

IV. CONCLUSION

This paper presents the method and error analysis for surface temperature measurement of an object in rotation (excitation winding of a synchronous hydro-generator) with the use of the industrial IR thermometer. A simplified mathematical model of the thermopile sensor has been described which was used to derive measurement error, and experimental results are presented. As the mathematical model shows, the correct temperature reading will be obtained if the interpolar surface irradiation can be neglected or cancelled.

Temperature change
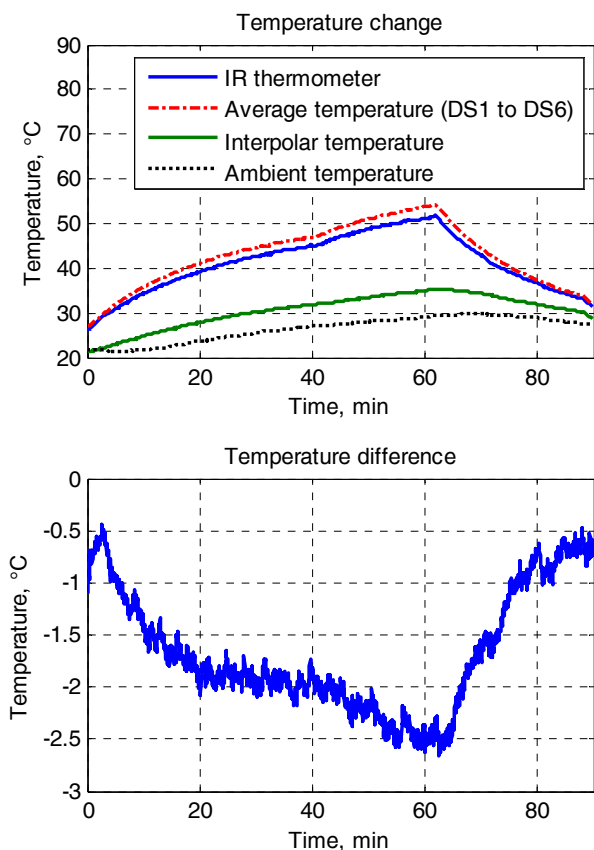

Temperature difference

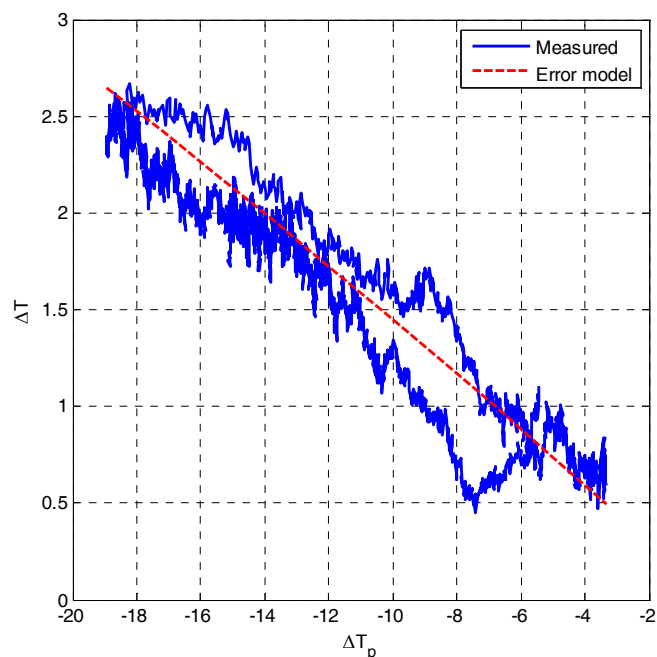Fig.20 – Heating and cooling in rotation, experiment 4

Fig.21 – Comparison of measured and modeled measurement error, experiment 4.

It is important to note that the previous works on the IR measurement in rotation include very fast IR cameras. This paper shows that industrial IR thermometer can be used and by setting the emissivity factor according to proposed methods or choosing a favorable point of view, satisfactory small measurement error can be achieved.

The accuracy of presented measurement method is satisfactory for its targeted application (determination of the dynamic limit in the P-Q diagram of a synchronous generator). Further research may include measurement on another synchronous machine, use of fast IR camera, a more detailed mathematical model of a thermometer or camera, the analysis of influence of the ambient temperature and machine ventilation on the measurement and measurement error, as well as application of this method to other rotating object or other machines (eg. synchronous turbo-generators, induction machines, PM synchronous machines etc.)

V. REFERENCES

[1] X. Maldague, "Theory and practice of infrared technology for nondestructive testing", John Wiley and Sons Inc, New York, 2001.

[2] W. Minkina, S. Dudzik, "Infrared Thermography: Errors and Uncertainties", Wiley, New York, 2009

[3] W. Minkina, S. Dudzik, "Simulation analysis of uncertainty of infrared camera measurement and processing path", *Measurement*, Volume 39 (2006.), Issue 8, Pages 758-763

[4] T. Astrita, G. Cardone, G. M. Carlomagno, C. Meola, "A survey on infrared thermography for convective heat transfer measurements" *Optics and Laser Technology* 32 (2000) 593–610.

[5] T. Astrita, G. Cardone, G. M. Carlomagno: "Infrared thermography an optical method in heat transfer and fluid flow visualization", *Optics and Laser in Engineering* 44 (2006) 261–281.

[6] M. Mori, L. Novak and M. Sekavcnik, "Measurements on rotating blades using IR thermography", *Exp Thermal Fluid Sci* 32(2): 387–396

[7] G. Zhi, T. G. Habetler, R. G. Harley, R. S. Colby, "A Sensorless Rotor Temperature Estimator for Induction Machines Based on a Current Harmonic Spectral Estimation Scheme," *Industrial Electronics, IEEE Transactions on* , vol.55, no.1, pp.407-416, Jan. 2008

[8] G. Zhi, T. G. Habetler, R. G. Harley, "A Complex Space Vector Approach to Rotor Temperature Estimation for Line-Connected Induction Machines With Impaired Cooling," *Industrial Electronics, IEEE Transactions on* , vol.56, no.1, pp.239-247, Jan. 2009

[9] G. Zhi, R. S. Colby, T. G. Habetler, R. G. Harley, "A Model Reduction Perspective on Thermal Models for Induction Machine Overload Relays," *Industrial Electronics, IEEE Transactions on* , vol.55, no.10, pp.3525-3534, Oct. 2008

[10] P. Zhang, L. Bin, T. G. Habetler, "A Remote and Sensorless Stator Winding Resistance Estimation Method for Thermal Protection of Soft-Starter-Connected Induction Machines," *Industrial Electronics, IEEE Transactions on* , vol.55, no.10, pp.3611-3618, Oct. 2008

[11] P. Zhang, Y. Duan, T. Habetler, B. Lu, "Magnetic Effects of DC Signal Injection on Induction Motors for Thermal Evaluation of Stator Windings," *Industrial Electronics, IEEE Transactions on* , vol.PP, no.99, pp.1, 0

[12] S. A. Merryman, R. M. Nelms, "Diagnostic technique for power systems utilizing infrared thermal imaging," *Industrial Electronics, IEEE Transactions on* , vol.42, no.6, pp.615-628, Dec 1995

[13] Mejuto, C.; Mueller, M.; Staton, D.; Mebarki, S.; Al-Khayat, N.; , "Thermal Modelling of TEFC Alternators," *IEEE Industrial Electronics, IECON 2006 - 32nd Annual Conference on* , vol., no., pp.4813-4818, 6-10 Nov. 2006
doi: 10.1109/IECON.2006.347908

[14] Mejuto, C.; Mueller, M.; Shanel, M.; Mebarki, A.; Reekie, M.; Staton, D.; , "Improved synchronous machine thermal modelling," *Electrical Machines, 2008. ICEM 2008. 18th International Conference on* , vol., no., pp.1-6, 6-9 Sept. 2008
doi: 10.1109/ICELMACH.2008.4799886

[15] R. Boutarfa, S. Harmand: "Local convective heat exchanges and flow structure in a rotor–stator system" *International Journal of Thermal Sciences* 42 (2003) 1129–1143

[16] G. Cardone, T. Astarita, G. M. Carlomagno, "Infrared heat transfer on the rotating disk", *Optical Diagnostics in Engineering* 1 (2) (1996) 1–7.

[17] C. Kral, et. al., "Rotor temperature estimation of squirrel-cage induction motors by means of a combined scheme of parameter estimation and a thermal equivalent model," *Industry Applications, IEEE Transactions on* , vol.40, no.4, pp. 1049- 1057, July-Aug. 2004

[18] M. Mori, L. Novak, M. Sekavcnik, e.t al.. "Application of IR thermography as a measuring method to study heat transfer on rotating surface", *Forschung Im Ingenieurwesen-Engineering Research* 72(1):1–10

[19] H. Budzier, M. Zimmerhackl, V. Krause, and G. Hoven, "High speed IR camera for contactless temperature measurement on rotating tires", *Proc. Sensor 99*, pp. 41-46, Vol. 1, 1999

[20] J. Pellé, S. Harmand, "Heat transfer study in a rotor-stator system air-gap with an axial inflow", *Applied Thermal Engineering 29* (2009), Pages 1532-1543

[21] M. Vražić, I. Gašparac, M. Pavlica, "Some Problems of Synchronous Hydro-Generator Temperature Measurement",: A.P.D.E.E. 2008, Coimbra, Portugal, Page(s): 1-4, September 2008

[22] I. Ilić, Z. Maljković, I. Gašparac et. al. "Methodology for Determining the Actual P-Q Diagram of a Hydrogenerators" *Journal of Energy*, Vol.56 No.2 pp. 141 - 181, February 2007

[23] A. Boglietti, A. Cavagnino, and D. Staton, "Determination of critical parameters in electrical machine thermal models" in *Conf. Rec. IEEE IAS Annu. Meeting*, New Orleans, LA, Sep. 2007, pp. 73–90.

[24] F. Marignetti, V. Delli Colli, Y. Coia, "Design of Axial Flux PM Synchronous Machines Through 3-D Coupled Electromagnetic Thermal and Fluid-Dynamical Finite-Element Analysis," *Industrial Electronics, IEEE Transactions on* , vol.55, no.10, pp.3591-3601, Oct. 2008

[25] Yunkai Huang, Jianguo Zhu, Youguang Guo, "Thermal Analysis of High-Speed SMC Motor Based on Thermal Network and 3-D FEA With Rotational Core Loss Included," *Magnetics, IEEE Transactions on* , vol.45, no.10, pp.4680-4683, Oct. 2009

[26] J. P. Bastos, M. F. R. R. Cabreira, N. Sadowsk, S. R. Arruda, S. L. Nau, "A thermal analysis of induction motors using a weak coupled modeling," *Magnetics, IEEE Transactions on* , vol.33, no.2, pp.1714-1717, Mar 1997

[27] C. Mejuto, M. Mueller, M. Shanel, A. Mebarki, and D. Staton, "Thermal modelling investigation of heat paths due to iron losses in synchronous machines" in *Proc. IEEE PEMD*, Apr. 2008, pp. 225–229

[28] A. Boglietti, A. Cavagnino, D. Staton, M. Shanel, M. Mueller, C. Mejuto, "Evolution and Modern Approaches for Thermal Analysis of Electrical Machines" *Industrial Electronics, IEEE Transactions on* , vol.56, no.3, pp.871-882, March 2009

[29] W. Li, D. Shuye, J. Huiyong, L. Yingli, "Numerical Calculation of Multicoupled Fields in Large Salient Synchronous Generator," *Magnetics, IEEE Transactions on* , vol.43, no.4, pp.1449-1452, April 2007

[30] N. Jaljal, J.-F. Trigeol; P. Lagonotte, "Reduced Thermal Model of an Induction Machine for Real-Time Thermal Monitoring," *Industrial Electronics, IEEE Transactions on* , vol.55, no.10, pp.3535-3542, Oct. 2008

[31] G. Traxler-Samek; R. Zickermann; A. Schwery, "Cooling Airflow, Losses, and Temperatures in Large Air-Cooled Synchronous Machines," *Industrial Electronics, IEEE Transactions on* , vol.57, no.1, pp.172-180, Jan. 2010

[32] D. G. Dorrell, "Combined Thermal and Electromagnetic Analysis of Permanent-Magnet and Induction Machines to Aid Calculation," *Industrial Electronics, IEEE Transactions on* , vol.55, no.10, pp.3566-3574, Oct. 2008

[33] S. Mezani; N. Takorabet, B. Laporte, "A combined electromagnetic and thermal analysis of induction motors", *Magnetics, IEEE Transactions on* , vol.41, no.5, pp. 1572- 1575, May 2005

[34] P. Mellor, D. Roberts, and D. Turner, "Lumped parameter thermal model for electrical machines of TEFC design" *Proc. Inst. Elect. Eng.*, vol. 138, no. 5, pp. 205–218, Sep. 1991.

[35] A. Boglietti, A. Cavagnino, M. Lazzari, and M. Pastorelli, "A simplified thermal model for variable-speed self-cooled industrial induction motor", *IEEE Trans. Ind. Appl.*, vol. 39, no. 4, pp. 945–952, Jul./Aug. 2003.

[36] J. F. Trigeol, Y. Bertin, and P. Lagonotte, "Thermal modeling of an induction machine through the association of two numerical approaches" *IEEE Trans. Energy Convers.*, vol. 21, no. 2, pp. 314–323, Jun. 2006.

[37] D. Staton, A. Boglietti, and A. Cavagnino, "Solving the more difficult aspects of electric motor thermal analysis in small and medium size industrial induction motors" *IEEE Trans. Energy Convers.*, vol. 20, no. 3, pp. 620–628, Sep. 2005.

[38] A. Di Gerlando, G. Foglia, and R. Perini, "Permanent magnet machines for modulated damping of seismic vibrations: Electrical and thermal modeling" *IEEE Trans. Ind. Electron.*, vol. 55, no. 10, pp. 3602–3610, Oct. 2008.

[39] A. Tenconi, F. Profumo, S. E. Bauer, and M. D. Hennen, "Temperatures evaluation in an integrated motor drive for traction applications" *IEEE Trans. Ind. Electron.*, vol. 55, no. 10, pp. 3619–3626, Oct. 2008.

[40] Mejuto, C.; Mueller, M.; Shanel, M.; Mebarki, A.; Staton, D.; , "Thermal modelling investigation of heat paths due to iron losses in synchronous machines," *Power Electronics, Machines and Drives, 2008. PEMD 2008. 4th IET Conference on* , vol., no., pp.225-229, 2-4 April 2008

[41] J. P. Holman, "Heat Transfer", McGraw-Hill Book Company, New York, 2010

[42] M. Kovačić, M Vražić, I. Gašparac, "Bluetooth wireless communication and 1-wire digital temperature sensors in synchronous machine rotor temperature measurement," *Power Electronics and Motion Control Conference (EPE/PEMC), 2010 14th International* , vol., no., pp.T7-25-T7-28, 6-8 Sept. 2010

[43] S. Stipetić, M. Kovačić, Z. Hanić, "The analysis of the infrared excitation winding surface temperature measurement on a synchronous hydro-generator in rotation," *Electrical Machines (ICEM), 2010 XIX International Conference on* , vol., no., pp.1-6, 6-8 Sept. 2010

VI. BIOGRAPHIES

Stjepan Stipetic was born in Ogulin, Croatia on February 2, 1985. He received M. Eng. degree in electrical engineering from the University of Zagreb, Croatia in 2008. Currently he is a Ph.D. student working as a junior researcher at the Department of Electric Machines, Drives and Automation, Faculty of Electrical Engineering and Computing, University of Zagreb. He is a member of IEEE and the Croatian National Committee of CIGRÉ.

Marinko Kovacic was born in Split, Croatia on June 2, 1985. He received M. Eng. degree in electrical engineering from the University of Zagreb, Croatia in 2009. Currently he is a Ph.D. student working as a junior researcher at the Department of Electric Machines, Drives and Automation, Faculty of Electrical Engineering and Computing, University of Zagreb.

Zlatko Hanic was born in Zagreb, Croatia on April 14, 1986. He received M. Eng. degree in electrical engineering from the University of Zagreb, Croatia in 2009. Currently he is a Ph.D. student working as a junior researcher at the Department of Electric Machines, Drives and Automation, Faculty of Electrical Engineering and Computing, University of Zagreb. He is member of IEEE.

Mario Vrazic was born in Zagreb, Croatia on September 16, 1971. He received his M.Sc. and PhD from University of Zagreb, Croatia in 2000 and 2005 respectively. Currently he is Assistant Professor at the Department of Electric Machines, Drives and Automation, Faculty of Electrical Engineering and Computing, University of Zagreb. He is a member of IEEE and the Croatian National Committee of CIGRÉ.